LANGMUIR

pubs.acs.org/Langmuir Article

Solvent-Dependent Adsorption of Perfluorosulfonated Ionomers on a Pt(111) Surface Using Atomic Force Microscopy

Ruttala Devivaraprasad and Takuya Masuda*

Cite This: https://dx.doi.org/10.1021/acs.langmuir.0c02023 Read Online

ACCESS | Metrics & More | Article Recommendations | Supporting Information

ABSTRACT: The adsorption behavior of perfluorosulfonated ionomers (PFSIs) on a Pt(111) surface in various solvents is investigated by in situ atomic force microscopy (AFM) and discussed on the basis of aggregation of PFSIs in the liquid phase. The AFM images show that, in an aqueous solution of PFSI (0.1 wt % Nafion + 99.9 wt % water), PFSI aggregates with a lateral size of 20−200 nm adsorb on the Pt(111) surface. In a PFSI solution containing a small amount of 1-propanol (0.1 wt % Nafion + 99.5 wt % water + 0.4 wt % 1-propanol), however, slightly smaller aggregates adsorb on the Pt(111) surface. Such solvent-dependent sizes of adsorbed aggregates are in reasonable agreement with apparent hydrodynamic radii of PFSIs in the corresponding solutions determined by dynamic light scattering (DLS) while assuming the formation of spherical aggregation. Interestingly, a step-terrace structure characteristic to a clean Pt(111) surface is observed in a propanol-rich PFSI solution (0.1 wt % Nafion + 44.45 wt % water + 55.45 wt % 1-propanol) but X-ray photoelectron spectroscopy clearly indicates the existence of fluorocarbon species at the Pt(111) surface, suggesting the formation of a smooth adsorbed layer of PFSIs in a lying down configuration. Absence of any features assignable to aggregates in DLS data suggests well-dispersion of PFSIs in such propanol-rich solution without aggregations. Thus, the adsorbed structure of PFSIs at Pt surfaces can be controlled by tuning the composition of mixed solvent, which affects the aggregation of PFSI in the liquid phase.

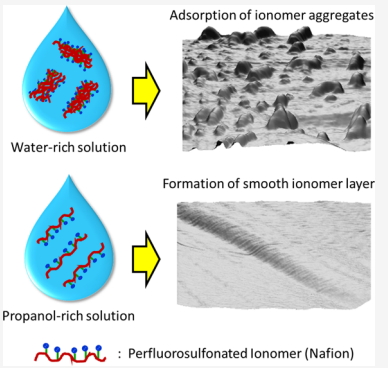

Downloaded via NATL RESEARCH COUNCIL CANADA on November 19, 2020 at 19:29:51 (UTC).
See https://pubs.acs.org/sharingguidelines for options on how to legitimately share published articles.

INTRODUCTION

Polymer electrolyte fuel cells (PEFCs) are one of the most promising power sources because of their high theoretical energy conversion efficiency and low environmental impact.[1] Nafion is one of the chief components used not only as a proton exchange membrane (PEM) but also as an ionomer in the catalyst layers (CLs) of membrane electrode assembly (MEA) which is manufactured by binding carbon-supported platinum catalysts mixed with ionomers on both sides of PEM.[2−5] Conventionally, the preparation of CLs involves the heterogeneous mixing of the ionomers with carbon-supported platinum catalysts in aqueous solutions, the homogeneous coating of a PEM with such catalyst ink, and drying/hot-pressing to yield a high ion conductivity and gas permeability.[6] Evidently, the adsorbed structure of ionomers on platinum catalysts significantly affects the oxygen/proton transport properties and electrocatalytic activity of CLs.[7] In this regard, controlling the adsorbed structure of the ionomers on carbon-supported platinum catalysts in the CLs is very important to improve the cell performance of PFECs.[8−13] However, tuning the ionomer adsorption in a controllable and scalable manner still lacks a practical methodology and remains a challenge because of a limited understanding of adsorbed structure at catalyst surfaces.

Recently, a few groups intensively attempted to control the microstructure of CLs by adding alcohols in catalyst inks.[11−22] Takahashi et al. investigated the influence of the microstructure of CLs tuned by using mixed solutions of 1-propanol and water on the cell performance through the structural observation by cryo-SEM and laser diffraction coupled with qualitative electrochemical analysis.[15] They found that catalyst inks prepared in three different solutions with different water/1-propanol ratios result in the formation of differently sized agglomerates of the Pt/C electrocatalysts interconnected by ionomers; cross-sectional cryo-SEM images indicated that larger agglomerates and pores were formed in CLs prepared from a water-rich solution, than those from an alcohol-rich solution. Such solvent-dependent microstructures can be interpreted based on the aggregations of ionomers and carbon-supported platinum catalysts in the liquid phase; ionomers are well-dispersed and relatively small agglomerates of carbon supports are dominant in the alcohol-rich solutions because of the amphiphilic behavior of alcohol,[23−25] whereas the size of the agglomerates was remarkably larger in the water-rich solution because of the segregation of hydrophobic fluorocarbon backbones and carbon surfaces.[12] Laser diffrac-

Received: July 9, 2020
Revised: October 19, 2020

© XXXX American Chemical Society

https://dx.doi.org/10.1021/acs.langmuir.0c02023
Langmuir XXXX, XXX, XXX−XXX

tion analyses of those catalyst inks used for fabricating the MEAs are indeed consistent with this interpretation. Moreover, it was shown that the agglomeration of carbon-supported platinum catalysts was substantially promoted in the presence of ionomers in solution.

They also investigated the effect of those microstructures on the oxygen reduction reaction (ORR) kinetic activity and oxygen transport property. The MEA from the water-rich ink displayed the best kinetic performance for ORR, whereas its mass transport property is rather poorer than one of those from the alcohol-rich catalyst inks probably due to the existence of large pores formed in the CLs which may cause the water accumulation and flooding. This result suggests that the addition of an appropriate amount of alcohol can control the microstructure of CLs, potentially leading to the improvement of mass transport property of MEAs.

Later Takahashi et al. employed cryo-TEM to visualize the microstructures of ionomers in the CLs.[17] Although aggregates of ionomers, carbon supports and carbon-supported platinum catalysts, as well as segregation of ionomers around the catalysts were clearly imaged with a high spatial resolution,[17] those microstructures might be compromised by the freezing procedures.[26,27] Thus, in situ techniques to image the adsorbed ionomers on platinum and carbon surfaces in a molecular/nanometer scale are strongly desired to achieve the better control of kinetic activity and mass transport property of MEAs. Several groups applied in situ experimental techniques[28−32] and theoretical methods[33−35] to the structural investigation of ionomers and proposed various morphologies under the influence of different solvents and thermal treatments.

AFM is a powerful technique to observe the adsorption process of ionomers onto solid surfaces in liquids. Previously, our group investigated the adsorption process of perfluorosulfonated ionomers (PFSIs) onto an atomically-flat HOPG surface[36] and the potential-dependent adsorption/desorption behavior of PFSIs at Pt and Au single-crystal surfaces using in situ AFM and other electrochemical methods.[37,38] Herein, we systematically monitored the adsorbed structure of PFSIs at Pt(111) surfaces using AFM in ionomer-containing solutions at various solvent compositions (water/1-propanol) as a model of the manufacturing process. 1-propanol was chosen as an additive in the present study not only because it is a fundamental system to understand the effect of solvent on structural development but it is practically employed in the manufacturing process. In propanol-free aqueous solutions, relatively large aggregates were adsorbed on the Pt(111) surface. When a small amount of 1-propanol was added in the ionomer-containing solutions, the size of adsorbed aggregates became somewhat smaller. Interestingly, in solutions containing 1-propanol as a major solvent species, a very smooth adsorbed layer was formed at the step-terrace structure characteristic to a bare Pt(111) surface. Thus, controlling the adsorbed structure of ionomer was demonstrated by tuning the solvent composition. Furthermore, the adsorbed structure of PFSIs at the Pt(111) surface was correlated with the aggregation of PFSIs in the liquid phase determined by using dynamic light scattering (DLS).

EXPERIMENTAL SECTION

Materials. Nafion dispersion D1021 (ionomer: 10−12 wt %, water: 87−90 wt %) and D2020 (ionomer: 20−22 wt %, water: 32−34 wt %, propanol: 44−46 wt %) procured from DuPont were used as PFSIs after dilution with ultrapure water (18.2 MΩ, TOC ∼ 4−5 ppb) from the Milli-Q system (Yamato, WQ-500) or a solvent mixture (ultrapure water + 1-propanol procured from Wako pure chemicals). The chemical structure and equivalent weight of PFSIs used in the present study are shown in Figure S1 and Table S1. A Pt(111) single-crystal surface (diameter: 10 mm, thickness: 5 mm, Surface Preparation Laboratory, The Netherlands) was used as a substrate for the AFM measurements.

Preparation of Pt(111) Substrate. A pristine Pt(111) surface was annealed at 1600 °C in 4% hydrogen and argon gas mixture for 1 h using an induction heater (AMBRELL, HOTSHOT 2 Ext.FF V4), prior to the AFM measurements. The cleanliness of the surface was also confirmed by the characteristic "butterfly features" in cyclic voltammograms of the Pt(111) surface recorded in a 0.05 M H_2SO_4 solution.

In Situ AFM Measurement. After obtaining the clean Pt(111) surface, the adsorption of PFSIs was monitored with Acoustic AC mode AFM (Tapping mode) using an Agilent 5500 AFM microscope (Agilent Technologies, USA) with a silicon nitride cantilever (PPP-FM, typical spring constant 2.8 N/m, resonance frequency 75 kHz; Nanosensors). Images were processed and analyzed by using Gwyddion and Image J software.[39,40] After a bare Pt(111) surface was imaged in a PFSI-free solvent (pure water or the mixed solvent of water/1-propanol) to confirm the cleanliness, the adsorbed structures of PFSIs at the Pt(111) surface were monitored by replacing the solvent with PFSI-containing solutions with different solvent compositions. The images were recorded over a period of ∼30 min in the scanning area of 1 μm × 1 μm. The compositions of PFSI solutions used in this study are given in Table 1. All of the concentrations throughout the paper were expressed in wt % unless otherwise specified.

Table 1. Compositions of the PFSI Solutions

	Nafion (%)	water (%)	propanol (%)	denoted as;
D1021	0.1	99.9		0.1 N + 99.9 W
D2020	0.1	99.5	0.4	0.1 N + 99.5 W + 0.4 P
D2020	0.1	44.45	55.45	0.1 N + 44.45 W + 55.45 P

DLS Measurement. DLS experiments were performed at 25 ± 0.1 °C using Dyno Pro Nanostar from Wyatt tech. In the DLS measurements, intensity correlation functions were obtained at 90°. The intensity time correlation functions $g^2(\tau)$ were fitted using an inverse Laplace procedure using the regularization algorithm in DYNAMICS which is DYNALS.[41] As-obtained translational diffusion coefficients were converted to hydrodynamic radii Rh, using the Stokes−Einstein equation.[29] Because the diluted low concentration solutions were employed, the effects of the viscosity and refractive index of the solvent on hydrodynamic radii were considered to be negligible.

RESULTS AND DISCUSSION

Surface Characterization of Pt(111) Using Voltammetry. Figure 1 shows a typical CV of Pt(111) electrodes obtained after induction heating, recorded in an argon-saturated 50 mM H_2SO_4 aqueous solution with a scan rate of 50 mV s^{-1}. Current waves due to the hydrogen underpotential deposition were observed in the potential range between −0.2 and 0.1 V with respect to a Ag/AgCl reference electrode. When the potential was swept positively from 0.1 V, a broad and a sharp reversible peak due to the adsorption/desorption of sulfate ions and their phase transformation were observed at around 0.2 and 0.24 V, respectively. These features are characteristic to a well-defined Pt(111) surface as reported previously.[42,43] The sharpness and

https://dx.doi.org/10.1021/acs.langmuir.0c02023
Langmuir XXXX, XXX, XXX−XXX

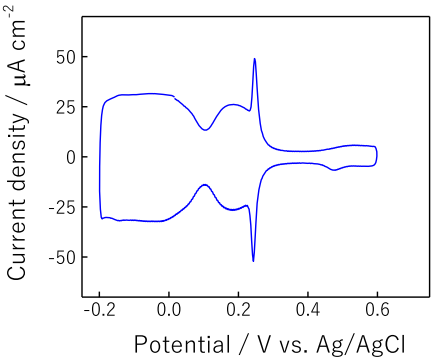

Figure 1. Cyclic voltammogram of the Pt(111) surface in an argon saturated 0.05 M H_2SO_4 solution recorded at a scan rate of 50 mV s^{-1}.

the symmetry of the voltammetric features of the Pt(111) surface are clear evidence of the surface cleanliness.

Observation of Ionomer Adsorption at the Pt(111) Surface Using AFM. At the pristine Pt(111) surface measured in pure water, a typical step-terrace structure devoid of any contamination was observed as shown in Figure 2a, confirming the formation of an atomically-flat clean surface. Figure 2b–d show the series of subsequently recorded AFM images of the Pt(111) surface in a solution containing 0.1 wt % Nafion and 99.9 wt % water (0.1 N + 99.9 W) prepared from D1021 at intervals ∼7, ∼15, and ∼30 min, respectively. Sparsely dispersed bright spots corresponding to the adsorbed PFSI aggregates with a lateral size of 20–200 nm and a height of a few nanometers were observed at the Pt(111) surface at ∼7 min (Figure 2b). Almost no noticeable differences were observed in the series of AFM images taken at time intervals (Figure 2b–d).

To examine the effect of 1-propanol, a freshly prepared Pt(111) surface was imaged in a solution of 0.1 wt % Nafion, 99.5 wt % water, and 0.4 wt % 1-propanol (0.1 N + 99.5 W + 0.4 P) prepared from D2020 after confirming the step-terrace structure of the Pt(111) surface in pure water (Figure 3a). At the initial stage (Figure 3b), aggregates with a lateral size of ∼20 nm and a height of a few nanometers, smaller than those in the propanol-free aqueous solution (Figure 2b–d), were observed at the Pt(111) surface. Although slightly larger aggregates with a lateral size of 50–100 nm were also observed with time (Figure 3b–d), they were not as large as those in the propanol-free solution. This suggests that the addition of 1-propanol into the PFSI solution facilitates the dispersion of ionomers in the liquid phase, leading to the adsorption of smaller aggregates. Trends in the effect of alcohol additive on the size of aggregates are in reasonable agreement with results reported by Takahashi et al.[15] The sizes of the adsorbed ionomer aggregates are latter discussed on the basis of the apparent size distribution in the liquid phase determined by DLS.

A significantly different behavior was observed when the concentration of 1-propanol was drastically increased in a solution of 0.1 wt % Nafion, 44.45 wt % water, and 55.45 wt % 1-propanol (0.1 N + 44.45 W + 55.45 P) prepared from D2020. Contrary to the images observed in the water-rich solutions (Figures 2b–d and 3b–d), a step-terrace structure characteristic to a bare Pt(111) surface was observed not only in the ionomer-free solvent mixture (Figure 4a) but also in the ionomer-containing solution (Figure 4b–d) without any remarkable adsorption of aggregates. AFM measurements with the scan area of ∼1 μm square and larger scan area of ∼10 μm square were applied to 9 different locations as shown in Figures S2 and S3, respectively, and a step-terrace structure without any aggregates was imaged at every location of the Pt(111) surface. One may consider that ionomer does not adsorb on the Pt(111) surface in such propanol-rich solutions. However, X-ray photoelectron spectroscopy (XPS) clearly showed C 1s and F 1s peaks assignable to fluorocarbon chains of adsorbed PFSIs at 293.5 and 685 eV, respectively, in the spectra of the Pt(111) surface immersed in the same D2020 ionomer solution (0.1 N + 44.45 W + 55.45 P) for 10 min followed by rinsing with water, as shown in Figures S4–S6. This suggests that a smooth adsorbed layer of PFSIs was formed at the Pt(111) surface in the propanol-rich solution without the adsorption of aggregates.

These observations in the propanol-containing (Figure 3) and propanol-rich solutions (Figure 4) prepared from D2020 were further verified using PFSI solutions prepared in identical compositions using D1021 as shown in Figures S7, S8 and Table S1. Trends in the effect of 1-propanol addition on the adsorbed structure of PFSI at the Pt(111) surface in the D1021-based solutions are in reasonable agreement with those

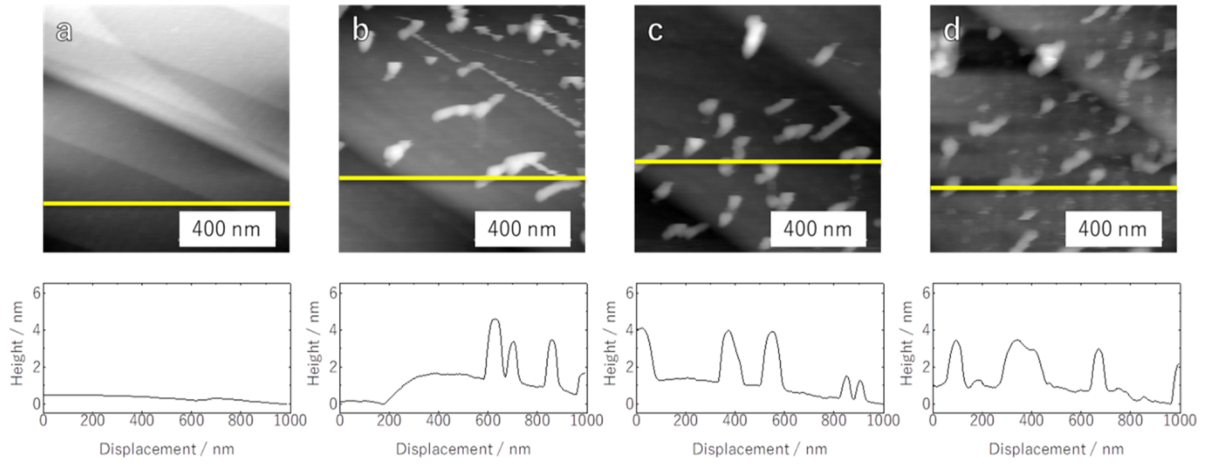

Figure 2. Series of AFM images of the Pt(111) surface recorded (a) in pure water and in the PFSI aqueous solution (0.1 N + 99.9 W from D1021) after (b) ∼7, (c) ∼15, and (d) ∼30 min.

https://dx.doi.org/10.1021/acs.langmuir.0c02023
Langmuir XXXX, XXX, XXX−XXX

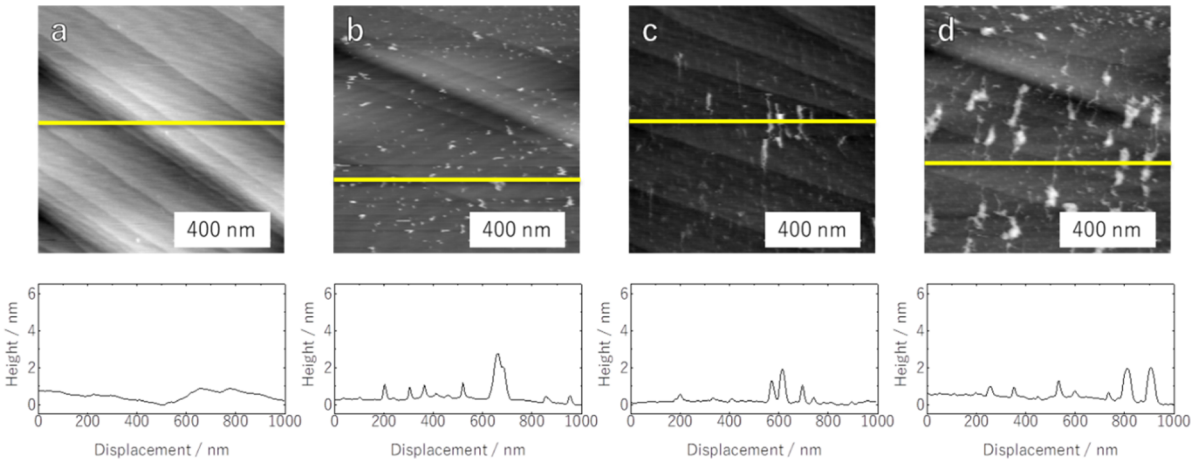

Figure 3. Series of AFM images of the Pt(111) surface recorded (a) in pure water and in the propanol-containing PFSI solution (0.1 N + 99.5 W + 0.4 P from D2020) after (b) ~7, (c) ~15, and (d) ~30 min.

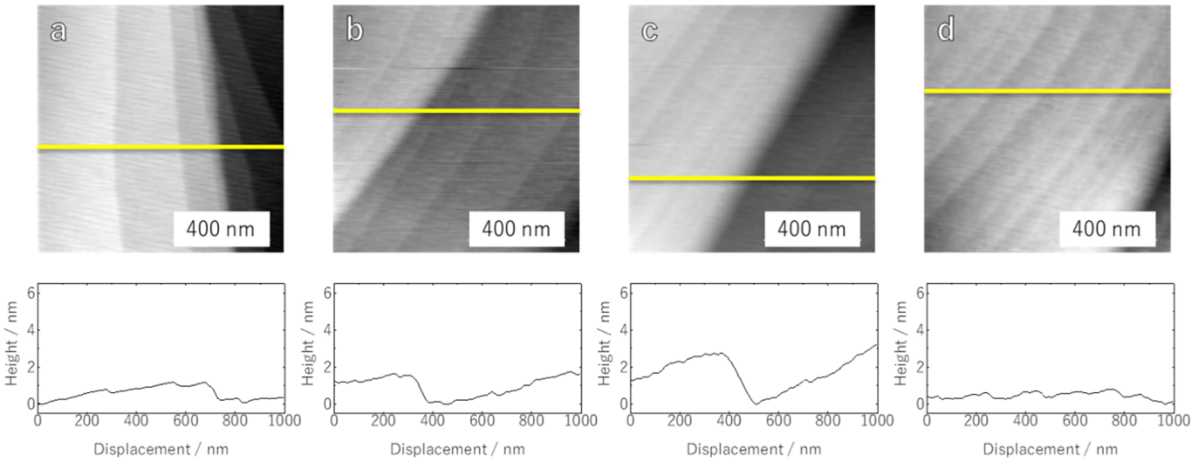

Figure 4. Series of AFM images of the Pt(111) surface recorded (a) in the solvent mixture (water/1-propanol) and in the propanol-rich PFSI solution (0.1 N + 44.45 W + 55.45 P from D2020) after (b) ~7, (c) ~15, and (d) ~30 min.

in the D2020-based solutions; the addition of small amount of 1-propanol as in (0.1 N + 99.5 W + 0.4 P) results in the formation of relatively smaller aggregates and propanol-rich solution as in (0.1 N + 44.45 W + 55.45 P) forms a relatively smooth ionomer layer at the Pt(111) surface. This suggests that the addition of 1-propanol into the PFSI solutions facilitates the dispersion of PFSI aggregates or formation of smooth ionomer layer depending on its composition, which is independent of the nature of the stock solution (D1021 or D2020). Thus, the adsorbed structures of ionomers at platinum surfaces were substantially controllable by tuning the solvent composition.

In order to roughly correlate the aggregation of PFSIs in the liquid phase to their adsorbed structure, their apparent hydrodynamic radii in the solutions with various compositions were determined by DLS in the later section, based on the assumption that all of the aggregates in solutions are spherical.

Investigation of the Ionomer Structure in Solutions Using DLS Measurement. Figure 5 shows typical autocorrelation function curves obtained from DLS measurements of the solutions used for in situ AFM. The PFSI solution containing a small amount of 1-propanol (0.1 N + 99.5 W + 0.4 P in Figure 5b) shows decay periods slightly faster than the propanol-free aqueous solution (0.1 N + 99.9 W in Figure 5a),

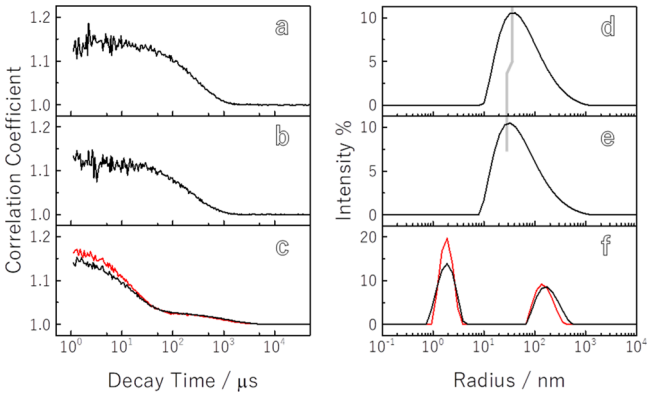

Figure 5. DLS autocorrelation function curves (a–c) and size distribution histograms (d–f) of the PFSI solutions with different compositions (a,d) 0.1 N + 99.9 W prepared from D1021, (b,e) 0.1 N + 99.5 W + 0.4 P, and (c,f) 0.1 N + 44.45 W + 55.45 P prepared from D2020. Data for the PFSI-free solvent mixture (water/1-propanol) was added in (c,f) by red lines for a comparison.

suggesting that the addition of 1-propanol indeed promotes the dispersion of PFSIs in the liquid phase. The size discrepancies of aggregates are more clearly evident in the size distribution histograms derived from the autocorrelation

https://dx.doi.org/10.1021/acs.langmuir.0c02023
Langmuir XXXX, XXX, XXX–XXX

function curves as shown in Figure 5d,e. Similar effect of the alcohol additive on the size of ionomer aggregates has been reported by Yamaguchi et al[29] In the alcohol-free aqueous solutions, the fluorocarbon backbones of PFSIs tend to aggregate because of the van der Waals interaction between fluorocarbon chains and repulsive interaction between water and hydrophobic fluorocarbon chains, leading to the formation of such relatively large aggregates ($\sim 10^2-10^3$ nm).[29,44] In contrast, amphiphilic molecules such as 1-propanol in the present case are considered to act as an aggregation prevention dispersants for PFSIs. This is consistent with the postulate derived from the AFM observations.

Although even faster decay was observed in the autocorrelation function curve of the solution containing 1-propanol as a major species (0.1 N + 44.45 W + 55.45 P in Figure 5c), it is almost identical to that of the ionomer-free solvent mixture. In addition, derived histograms (Figure 5f) are also almost the same, implying that the aggregation of PFSIs was effectively inhibited in the propanol-rich solution. Thus, a smooth adsorbed layer of PFSIs was formed at the Pt(111) surface without the formation of aggregates, from the propanol-rich solution containing well-dispersed PFSIs. Tokumasu et al. performed coarse-grained molecular dynamics simulations of similar systems and revealed that, at low ionomer concentration (≤5.0 wt %), the ionomer forms smaller and thinner aggregates with increasing 1-propanol fractions.[33,34] Moreover, excess addition of 1-propanol inhibits the aggregation and promotes the dispersion of ionomers in solutions.[34] These theoretical studies strongly support our AFM observations verified using DLS measurements.

It is noted that a bimodal size distribution at around 1−2 nm and 100−200 nm was observed not only in a histogram of the propanol-rich PFSI solution (0.1 N + 44.45 W + 55.45 P, black curve in Figure 5f) but also in that of the PFSI-free solvent mixture (water/1-propanol, red curve in Figure 5f). The former peak is considered to be due to an artifact because it is almost the smallest size limit of the instrument. The latter peak is attributable to mesoscale inhomogeneities which can be formed in aqueous solutions containing organic substances, such as amines, alcohols, and ethers.[45]

CONCLUSIONS

Solvent dependent structure of adsorbed PFSIs at a Pt(111) surface was investigated in various solutions containing PFSI, water, and 1-propanol at different compositions, as a model of the manufacturing process of CLs for PEFCs. The addition of a small amount of amphiphilic 1-propanol facilitates the dispersion of PFSIs in the liquid phase, resulting in the adsorption of smaller aggregates on the Pt(111) surface. Observation of the step-terrace structure characteristic to a clean Pt(111) surface in the PFSI solutions containing 1-propanol as a major species and detection of fluorocarbon species by XPS indicate the formation of a smooth adsorbed layer of PFSIs presumably in a lying down configuration on the Pt(111) surface without any remarkable aggregates. Thus, the structural integrity of ionomers at the surface of platinum catalysts can be controlled by tuning the solvent composition and appropriate blending of a few different solvents can improve the cell performance of PEFCs.

ASSOCIATED CONTENT

Supporting Information

The Supporting Information is available free of charge at https://pubs.acs.org/doi/10.1021/acs.langmuir.0c02023.

AFM images of the Pt(111) surfaces recorded in various solutions and XPS data of the Pt(111) surface immersed in the solution (0.1 N + 44.45 W + 55.45 P) for 10 min, followed by rinsing with water (PDF)

AUTHOR INFORMATION

Corresponding Author

Takuya Masuda − *Surface Chemical Analysis Group, Research Center for Advanced Measurement and Characterization, National Institute for Materials Science (NIMS), Tsukuba, Ibaraki 305-0044, Japan;* orcid.org/0000-0001-7462-2177; Phone: +81-29-860-4971; Email: MASUDA.Takuya@nims.go.jp

Author

Ruttala Devivaraprasad − *Surface Chemical Analysis Group, Research Center for Advanced Measurement and Characterization, National Institute for Materials Science (NIMS), Tsukuba, Ibaraki 305-0044, Japan*

Complete contact information is available at: https://pubs.acs.org/10.1021/acs.langmuir.0c02023

Notes

The authors declare no competing financial interest.

ACKNOWLEDGMENTS

We thank Mrs. Tsuruta and Kurono (Shoko Science) for a fruitful discussion. The present work was supported by the New Energy and Industrial Technology Development Organization (NEDO), Japan.

REFERENCES

(1) Steele, B. C. H.; Heinzel, A. Materials for Fuel-Cell Technologies. *Nature* **2001**, *414*, 345−352.

(2) Litster, S.; McLean, G. PEM Fuel Cell Electrodes. *J. Power Sources* **2004**, *130*, 61−76.

(3) Debe, M. K. Electrocatalyst Approaches and Challenges for Automotive Fuel Cells. *Nature* **2012**, *486*, 43−51.

(4) Diat, O.; Gebel, G. Proton Channels. *Nat. Mater.* **2008**, *7*, 13−14.

(5) Lopez-Haro, M.; Guétaz, L.; Printemps, T.; Morin, A.; Escribano, S.; Jouneau, P.-H.; Bayle-Guillemaud, P.; Chandezon, F.; Gebel, G. Three-Dimensional Analysis of Nafion Layers in Fuel Cell Electrodes. *Nat. Commun.* **2014**, *5*, 1−6.

(6) Holdcroft, S. Fuel Cell Catalyst Layers: A Polymer Science Perspective. *Chem. Mater.* **2014**, *26*, 381−393.

(7) Kusoglu, A.; Weber, A. Z. New Insights into Perfluorinated Sulfonic-Acid Ionomers. *Chem. Rev.* **2017**, *117*, 987−1104.

(8) Shin, S.-J.; Lee, J.-K.; Ha, H.-Y.; Hong, S.-A.; Chun, H.-S.; Oh, I.-H. Effect of the Catalytic ink Preparation Method on the Performance of Polymer Electrolyte Membrane Fuel cells. *J. Power Sources* **2002**, *106*, 146−152.

(9) Ma, S.; Chen, Q.; Jogensen, F.; Stein, P.; Skou, E. 19F NMR Studies of Nafion^{TM} Ionomer Adsorption on PEMFC Catalysts and Supporting Carbons. *Solid State Ionics* **2007**, *178*, 1568−1575.

(10) Xu, F.; Zhang, H.; Ilavsky, J.; Stanciu, L.; Ho, D.; Justice, M. J.; Petrache, H. I.; Xie, J. Investigation of a Catalyst Ink Dispersion Using Both Ultra-Small-Angle X-Ray Scattering and Cryogenic TEM. *Langmuir* **2010**, *26*, 19199−19208.

(11) Ngo, T. T.; Su, P. H.; Yu, T. L. Conformation of Nafion Molecules in Dilute Isopropyl Alcohol/Water Mixture Solutions. *Proceedings IWNA 2011, November 10−12, 2011, Vung Tau, Vietnam*, 2011, AMN-005-P (d); pp 10−13.
(12) Ngo, T. T.; Yu, T. L.; Lin, H.-L. Influence of the Composition of Isopropyl Alcohol/Water Mixture Solvents in Catalyst Ink Solutions on Proton Exchange Membrane Fuel Cell Performance. *J. Power Sources* **2013**, *225*, 293−303.
(13) Ngo, T. T.; Yu, T. L.; Lin, H.-L. Nafion-based Membrane Electrode Assemblies Prepared From Catalyst inks Containing Alcohol/water Solvent Mixtures. *J. Power Sources* **2013**, *238*, 1−10.
(14) Shibayama, M.; Matsunaga, T.; Kusano, T.; Amemiya, K.; Kobayashi, N.; Yoshida, T. SANS Studies on Catalyst Ink of Fuel Cell. *J. Appl. Polym. Sci.* **2014**, *131* 39842. DOI: 10.1002/app.39842.
(15) Takahashi, S.; Mashio, T.; Horibe, N.; Akizuki, K.; Ohma, A. Analysis of the Microstructure Formation Process and Its Influence on the Performance of Polymer Electrolyte Fuel-Cell Catalyst Layers. *ChemElectroChem* **2015**, *2*, 1560−1567.
(16) Park, Y.-C.; Tokiwa, H.; Kakinuma, K.; Watanabe, M.; Uchida, M. Effects of Carbon Supports on Pt Distribution, Ionomer Coverage and Cathode Performance for Polymer Electrolyte Fuel Cells. *J. Power Sources* **2016**, *315*, 179−191.
(17) Takahashi, S.; Shimanuki, J.; Mashio, T.; Ohma, A.; Tohma, H.; Ishihara, A.; Ito, Y.; Nishino, Y.; Miyazawa, A. Observation of Ionomer in Catalyst ink of Ploymer electrolyte Fuel cell using Cryogenic Trasmission Electron Microscopy. *Electrochim. Acta* **2017**, *224*, 178−185.
(18) Sharma, R.; Andersen, S. M. Zoom in Catalyst/Ionomer Interface in Polymer Electrolyte Membrane Fuel Cell Electrodes: Impact of Catalyst/Ionomer Dispersion Media/Solvent. *ACS Appl. Mater. Interfaces* **2018**, *10*, 38125−38133.
(19) Uchida, M.; Aoyama, Y.; Eda, N.; Ohta, A. Investigation of the Microstructure in the Catalyst Layer and Effects of Both Perfluorosulfonate Ionomer and PTFE-Loaded Carbon on the Catalyst Layer of Polymer Electrolyte Fuel Cells. *J. Electrochem. Soc.* **1995**, *142*, 4143.
(20) Uchida, M.; Aoyama, Y.; Eda, N.; Ohta, A. New Preparation Method for Polymer-Electrolyte Fuel Cells. *J. Electrochem. Soc.* **1995**, *142*, 463.
(21) Xie, Z.; Zhao, X.; Adachi, M.; Shi, Z.; Mashio, T.; Ohma, A.; Shinohara, K.; Holdcroft, S.; Navessin, T. Fuel Cell Cathode Catalyst Layers from "Green" Catalyst Inks. *Energy Environ. Sci.* **2008**, *1*, 184−193.
(22) Kishi, M.; Tanaka, M.; Mori, T. Preparation Procedure for the Electrode Slurries of Polymer Electrolyte Fuel Cells Utilizing the Irreversibility of Ionomer Adsorption onto Pt-C Particles. *J. Ceram. Soc. Jpn.* **2019**, *127*, 942−951.
(23) Malek, K.; Eikerling, M.; Wang, Q.; Navessin, T.; Liu, Z. Self-Organization in Catalyst Layers of Polymer Electrolyte Fuel Cells. *J. Phys. Chem. C* **2007**, *111*, 13627−13634.
(24) Malek, K.; Mashio, T.; Eikerling, M. Microstructure of Catalyst Layers in PEM Fuel Cells Redefined: A Computational Approach. *Electrocatalysis* **2011**, *2*, 141−157.
(25) Mashio, T.; Ohma, A.; Tokumasu, T. Molecular Dynamics Study of Ionomer Adsorption at a Carbon Surface in Catalyst Ink. *Electrochim. Acta* **2016**, *202*, 14−23.
(26) Zhang, L.; Li, P.; Li, D.; Guo, S.; Wang, E. Effect of Freeze-Thawing on Lipid Bilayer-Protected Gold Nanoparticles. *Langmuir* **2008**, *24*, 3407−3411.
(27) Ramirez, M. I.; Amorim, M. G.; Gadelha, C.; Milic, I.; Welsh, J. A.; Freitas, V. M.; Nawaz, M.; Akbar, N.; Couch, Y.; Makin, L.; Cooke, F.; Vettore, A. L.; Batista, P. X.; Freezor, R.; Pezuk, J. A.; Rosa-Fernandes, L.; Carreira, A. C. O.; Devitt, A.; Jacobs, L.; Silva, I. T.; Coakley, G.; Nunes, D. N.; Carter, D.; Palmisano, G.; Dias-Neto, E. Technical challenges of working with extracellular Vesicles. *Nanoscale* **2018**, *10*, 881−906.
(28) Welch, C.; Labouriau, A.; Hjelm, R.; Orler, B.; Johnston, C.; Kim, Y. S. Nafion in Dilute Solvent Systems: Dispersion or Solution? *ACS Macro Lett.* **2012**, *1*, 1403−1407.
(29) Yamaguchi, M.; Matsunaga, T.; Amemiya, K.; Ohira, A.; Hasegawa, N.; Shinohara, K.; Ando, M.; Yoshida, T. Dispersion of Rod-like Particles of Nafion in Salt-Free Water/1-Propanol and Water/Ethanol Solutions. *J. Phys. Chem. B* **2014**, *118*, 14922−14928.
(30) Yamaguchi, M.; Terao, T.; Ohira, A.; Hasegawa, N.; Shinohara, K. Size and Shape of Nafion Particles in Water after High-Temperature Treatment. *J. Polym. Sci.: Polym. Phys.* **2019**, *57*, 813−818.
(31) Gao, X.; Yamamoto, K.; Hirai, T.; Uchiyama, T.; Ohta, N.; Takao, N.; Matsumoto, M.; Imai, H.; Sugawara, S.; Shinohara, K.; Uchimoto, Y. Morphology Changes in Perfluorosulfonated Ionomer from Thickness and Thermal Treatment Conditions. *Langmuir* **2020**, *36*, 3871−3878.
(32) Gupit, C. I.; Li, X.; Maekawa, R.; Hasegawa, N.; Iwase, H.; Takata, S.; Shibayama, M. Nanostructures and Viscosities of Nafion Dispersions in Water/Ethanol from Dilute to Concentrated Regimes. *Macromolecules* **2020**, *53*, 1464−1473.
(33) Mabuchi, T.; Tokumasu, T. Ionomer Dispersions in Water/Alcohol Solutions by Coarse-Grained Molecular Dynamics. *ECS Trans.* **2017**, *80*, 577−581.
(34) Mabuchi, T.; Huang, S.-F.; Tokumasu, T. Dispersion of Nafion Ionomer Aggregates in 1-Propanol/Water Solutions: Effects of Ionomer Concentration, Alcohol Content, and Salt Addition. *Macromolecules* **2020**, *53*, 3273−3283.
(35) Tarokh, A.; Karan, K.; Ponnurangam, S. Atomistic MD Study of Nafion Dispersions: Role of Solvent and Counterion in the Aggregate Structure, Ionic Clustering, and Acid Dissociation. *Macromolecules* **2020**, *53*, 288−301.
(36) Masuda, T.; Naohara, H.; Takakusagi, S.; Singh, P. R.; Uosaki, K. Formation and Structure of Perfluorosulfonated Ionomer Thin Film on a Graphite Surface. *Chem. Lett.* **2009**, *38*, 884−885.
(37) Masuda, T.; Sonsudin, F.; Singh, P. R.; Naohara, H.; Uosaki, K. Potential-Dependent Adsorption and Desorption of Perfluorosulfonated Ionomer on a Platinum Electrode Surface Probed by Electrochemical Quartz Crystal Microbalance and Atomic Force Microscopy. *J. Phys. Chem. C* **2013**, *117*, 15704−15709.
(38) Masuda, T.; Ikeda, K.; Uosaki, K. Potential-Dependent Adsorption/Desorption Behavior of Perfluorosulfonated Ionomer on a Gold Electrode Surface Studied by Cyclic Voltammetry, Electrochemical Quartz Microbalance, and Electrochemical Atomic Force Microscopy. *Langmuir* **2013**, *29*, 2420−2426.
(39) Nečas, D.; Klapetek, P. G. An Open-Source Software for SPM Data Analysis. *Cent. Eur. J. Phys.* **2012**, *10*, 181−188.
(40) Abràmoff, M. D.; Magalhães, P. J.; Ram, S. J. Image Processing with ImageJ. *Biophotonics Int.* **2004**, *11*, 36−42.
(41) Goldin, A. A. Dynals v1.0 white paper (online). 2002, available at: http://www.softscientific.com/science/WhitePapers/dynals1/dynals100.htm (last updated in March 2002).
(42) Wang, J. X.; Markovic, N. M.; Adzic, R. R. Kinetic Analysis of Oxygen Reduction on Pt(111) in Acid Solutions: Intrinsic Kinetic Parameters and Anion Adsorption Effects. *J. Phys. Chem. B* **2004**, *108*, 4127−4133.
(43) Markovic, N.; Gasteiger, H.; Ross, P. N. Kinetics of Oxygen Reduction on Pt(Hkl) Electrodes: Implications for the Crystallite Size Effect with Supported Pt Electrocatalysts. *J. Electrochem. Soc.* **1997**, *144*, 1591.
(44) Doo, G.; Lee, J. H.; Yuk, S.; Choi, S.; Lee, D.-H.; Lee, D. W.; Kim, H. G.; Kwon, S. H.; Lee, S. G.; Kim, H.-T. Tuning the Ionomer Distribution in the Fuel Cell Catalyst Layer with Scaling the Ionomer Aggregate Size in Dispersion. *ACS Appl. Mater. Interfaces* **2018**, *10*, 17835−17841.
(45) Subramanian, D.; Anisimov, M. A. Resolving the Mystery of Aqueous Solutions of Tertiary Butyl Alcohol. *J. Phys. Chem. B* **2011**, *115*, 9179−9183.

https://dx.doi.org/10.1021/acs.langmuir.0c02023
Langmuir XXXX, XXX, XXX−XXX